Journal of Building Engineering 30 (2020) 101279

Contents lists available at ScienceDirect

Journal of Building Engineering

journal homepage: http://www.elsevier.com/locate/jobe

# Building thermal load management through integration of solar assisted absorption and desiccant air conditioning systems: A model-based simulation-optimization approach

Muhammad Farhan Habib [a], Muzaffar Ali [b,*], Nadeem Ahmed Sheikh [c], Abdul Waheed Badar [d], Sajid Mehmood [e]

[a] Mechanical Engineering Department, University of Engineering and Technology, Taxila, Pakistan
[b] Energy Engineering Department, University of Engineering and Technology, Taxila, Pakistan
[c] Mechanical Engineering Department, International Islamic University, Islamabad, Pakistan
[d] Mechanical Engineering Department, HITEC University, Taxila, Pakistan
[e] Mechanical Engineering Department, University of Engineering and Technology, Lahore, Pakistan

ARTICLE INFO

*Keywords:*
Integrated cooling system
Solid desiccant
TRNSYS
GenOpt
Solar energy
Absorption system

ABSTRACT

Performance of standalone air-conditioning systems is affected while simultaneously handling both sensible and latent building loads. Model-based simulation and optimization is one of the best ways to analyze system's performance under load fluctuations at the initial design stages. Therefore, in the current study, seasonal transient simulations of an Integrated Absorption Desiccant System are carried out using TRNSYS to handle sensible (10.94 kW peak) and latent (4.44 kW peak) cooling load separately. Radiant cooling with chilled water from an absorption chiller mainly handles sensible cooling load, while the latent load is achieved by a solid desiccant dehumidification system. Initially, key components of the system are modeled in TRNSYS including a flat plate solar collector system, desiccant wheel, heat recovery wheel, and absorption chiller. Afterwards, the integrated model is coupled with GenOpt to optimize the solar fraction and thermal coefficient of performance by varying collector area, flow rate in the collector loop, flow rate in load side loop, and volume of storage tank. The resulted optimized value of solar fraction is 57.50%, and $COP_{th}$ is 0.55 for standalone absorption system, whereas the solar fraction of 56.20%, $COP_{th}$ of 1.52 are achieved for IADS. In addition, the effects of load variation in terms of sensible to latent load ratio on regeneration heat required for both IADS and conventional desiccant system are also analyzed. A critical value of load ratio of 0.75 is also observed in terms of heat regeneration requirements to compare the both systems. The proposed approach and analysis will be very helpful for HVAC designers for optimal system performance through separate load handling, especially at the initial design stage.

## 1. Introduction

Due to the increasing trend in worldwide energy demand, fossil fuels such as oil, gasoline diesel fuel, natural gas, and coal are depleting rapidly. The rate of consumption of fossil fuels is affected by increase in population and energy intensive living standard of people [1].

Global warming problems that include greenhouse effect, depletion of the ozone layer, acid rain, and some other generalized environmental pollution are also caused by the combustion of fossil fuels. To mitigate all these problems of climate change, solar energy is an alternative choice to fulfill world energy demands [2].

Building sector uses approximately 115 EJ energy globally which is 32% of world final energy demand in which 24% share is of residential and 8% of commercial buildings. Moreover, around 30% emissions due to $CO_2$ [3]. Around 50% of global energy consumption in a building is used for space heating and cooling together [4].

Various heating and cooling systems are commercially used which are driven or assisted by renewable energy resources [5]. Solar Absorption, solar desiccant, and solar adsorption systems are the best examples of such systems. However, as globally demand for thermal comfort is increasing rapidly, so there is a need for sustainable air conditioning systems. To achieve thermal comfort, cooling the air below dew point temperature is essential for dehumidifying air in conventional air conditioning systems [6]. The hybrid desiccant-absorption system is one of the best sustainable cooling systems because hybrid system is

* Corresponding author.
*E-mail addresses:* muzaffar.ali@uettaxila.edu.pk, muzaffarali79@yahoo.com (M. Ali).

https://doi.org/10.1016/j.jobe.2020.101279
Received 15 September 2019; Received in revised form 10 February 2020; Accepted 12 February 2020
Available online 15 February 2020

**Nomenclature**

| | |
|---|---|
| Ac | Collector area ($m^2$) |
| $a_o$, $a_1$, $a_2$ | optical efficiency, first order heat loss coefficient, Second order heat loss coefficient |
| COP | Coefficient of performance |
| $C_p$ | Specific heat of fluid (kJ/kg °C) |
| DAC | Conventional desiccant air-conditioning |
| E | Energy (kW) |
| F1, F2 | Iso-potential lines of wave propagation in desiccant wheel |
| *G* | Available global solar radiation on the collector surface ($W/m^2$) |
| $H_v$ | Heat of vaporization of water (kJ/kg) |
| h | Enthalpy (kJ/kg.K) |
| HJ | Hooke-Jeeves |
| HX | Heat Exchanger |
| $\dot{m}$ | Mas flow rate (Kg/s) |
| OF | Objective Function |
| Q | Thermal energy (kW) |
| SF | Solar fraction (%) |
| T | Temperature (°C) |
| $\Delta T$ | Temperature difference between the inlet fluid temperature and ambient temperature (°C) |
| $V_t$ | Volume of storage tank ($m^3$) |

*Greek Letter*

| | |
|---|---|
| ω | Absolute Humidity (g/kg) |
| ε | Effectiveness |
| $\eta$ | Collector Efficiency |

*Subscripts*

| | |
|---|---|
| a | Air |
| abs | Absorption |
| amb | Ambient |
| *aux* | Auxiliary |
| b | Boiler |
| c | Collector |
| chw | Chilled water |
| cw | Cooling water |
| d | Desiccant |
| ec | Evaporative Cooler |
| elc | Electric |
| g | Generator |
| i | In |
| lat | Latent |
| o | Out |
| *ovr* | Overall |
| p | Process |
| r | return |
| reg | Regeneration |
| sen | Sensible |
| sol | Solar |
| s | Sup |
| sp | Set Point |
| th | Thermal |
| tot | Total |
| w | Water |
| z | Zone |

more efficient than a standalone system. The reason is that, in case of a hybrid absorption-desiccant system, sensible load and latent loads are handled separately. In such systems, desiccant system handles the latent load and absorption system caters the sensible load [7]. So, an efficient thermal load management can be achieved using such an integration.

Hot and humid climates were focused by many researchers to indicate the benefits of solid desiccant-based hybrid systems [8–10]. In recent studies, solid desiccant system integrated with vapor compression system was modeled in TRNSYS and results were compared with experimental setup to investigate its performance in hot and humid climate [11]. Three different configurations of solid desiccant integrated system were studied and it was found that the energy saving with vapor compression integration was 50.6% [12]. Similarly, it was investigated experimentally that the latent load handling was improved and the system resulted in higher $COP_{th}$ by the hybridization of desiccant system with vapor compression system compared to a standalone vapor compression system [13]. Moreover, it was revealed that for hot and humid climate the COP of such hybrid system was 12.4% higher than the conventional system [14]. Integrated cogeneration air conditioning system was studied experimentally and compared with another cogeneration system. It was determined that the performance of the system affected by changing the regeneration temperature [15]. The thermal performance of hybrid desiccant system increased by decreasing the required temperature for regeneration purpose [16]. Around 34.97% prime energy savings was achieved by integrating compression-absorption with liquid desiccant system [17]. Moreover, it was also studied that for moderate climates, integration of a desiccant system with natural water is enough to handle sensible load [18]. Whereas, for hot and humid climate, a geothermal based desiccant integrated system was shown to be a viable option [19]. In another study, it was examined that a solar assisted desiccant cooling system for climate of Hong Kong resulted substantial potential for up to 17.7%–18% energy saving [20]. It was studied that the solar assisted desiccant system was optimized with respect to minimizing regeneration temperature and achieved $COP_{th}$ of 1.6 for optimal values of parameters [21]. A heating and cooling system was optimized using heuristic-deterministic algorithm for error function evaluation to maximize the performance of the system [22]. An experimental study of desiccant system integrated with vapor compression unit was carried out to check the saving potential of the integrated system. It was investigated that the system saved 37.5% electricity to maintain 30 °C supply temperature and 55% relative humidity when regenerated at 80 °C [23].

Hybridization in form of multiple system configurations were also analyzed by many researchers. A study was focused on major three points: (1) real systems coupled with solar thermal source (2) solar air collectors for the heating source in desiccant cooling system, and (3) different configurations of system and the three performances under different climatic variation were discussed [24]. The humid climate conditions of UAE were considered to monitor the performance of two system configurations (ventilation and recirculation) of desiccant cooling system and efficient indirect evaporative cooler i.e. Maisotsenko cooler. Average COP of Ventilation configuration was 0.25 and of recirculation configuration was 0.2713 and share of solar energy for the both was 32.2% and 36.5%, respectively [25]. Transient simulations of six different configurations of a solar assisted desiccant cooling system were conducted and resulted in 35.2% energy saving for year around operation [26]. A separate load handling was performed experimentally using solar assisted desiccant air conditioning system integrated with Maisotsenko cycle. It was observed that the system achieved solar fraction of 70%, COP of 0.91 and average cooling capacity 3.78 kW [27]. Many researchers optimized solar assisted standalone desiccant systems as well as integrated systems using different algorithms and objective functions [28–31]. In a simulation study using TRNSYS, a desiccant system proved efficient when integrated Maisotsenko cycle (M-Cycle) indirect evaporative cooler which resulted in $COP_{th}$ of 0.73 [32].

Other than human comfort, many studies were also related to the

applications of desiccant integrated systems for non-human thermal comfort like for storage of dry fruits, agriculture products storage, thermal comfort for livestock [33–36] which showed wide range to applicability of these systems.

Although there are many studies in which desiccant systems are tested, improved and compared with their counterparts, however only a very few studies can be found on the hybrid systems configurations using desiccant system with absorption system especially for separate load handling. There is a considerable knowledge gap to work on a such kind of system hybridization for separate load handling. The proposed integration of two systems of mature technologies and the resultant model is fully capable to handle sensible and latent load separately. Thus, the analysis is carried out to compare the integration with standalone absorption and desiccant system as baseline which resulted significant energy efficiency improvements. In the current study, model-based transient simulations are performed and subsequently the optimization is carried out using Hooke-Jeeves algorithm with properly constrained system model to maximize solar fraction and $COP_{th}$ of the integrated system. Moreover, the proposed integrated system performance is also investigated by varying sensible to latent load ratios. Based on the critical value of the ratio and regeneration heat requirements, the improved air-conditioning system is resulted.

## 2. Description of the integrated system

In the current work, the proposed integrated absorption desiccant system (IADS) consists of three sub-systems, (i) solar heating system, (ii) desiccant dehumidification system, and (iii) absorption chiller. Solar thermal source is used as a driving force for both IADS and absorption chiller as shown in Fig. 1.

The main challenge of a DAC system is that some moisture is added to the air due to direct contact between air and water during cooling. So, an indirect type cooling coil heat exchanger unit coupled with absorption chiller is used in place of a direct evaporative cooler. So, sensible load is handled by absorption chiller and latent load is managed by the desiccant wheel. From point 1 to 3, the processes are similar to a DAC system, whereas from point 3 to 4, only sensible cooling is involved with constant humidity ratio. Furthermore, from point 7 to 8, the desiccant wheel is regenerated through hot water from the solar thermal system.

The psychrometric representation of all related processes from point 1 to 9 are shown on psychrometric chart in Fig. 2. It is to be noted that the processes from point 1 to 2 and 2 to 3 would be same for both DAC and IADS. The basic difference between DAC and IADS will be the process from point 3 to 4. For DAC systems, the process 3 to 4 is cooling and humidification but in case of IADS the process is just sensible cooling as no moisture is added. Moreover, points 4 and 5 are room supply and return air conditions, respectively.

## 3. Development of simulation model of the integrated system

TRNSYS is a simulation package and is used for the analysis of dynamic systems and energy systems on transient basis [37]. For every component of TRNSYS there are a set of mathematical equations that are being solved through a solver. TRNSYS works on basis of its two parts. The first part is termed as its engine and second part is its components library including 150 models. The first part of the TRNSYS critically reads input file of each component of the model then processes it, solve it iteratively and finds the convergence of variables of the system according to selected criteria. Some utilities are provided by the first part that determine invert matrices and thermophysical properties.

In the current study, all the system components (solar collector, storage tank, auxiliary boiler, cooling tower, air handling unit, dehumidification wheel, pumps) were modeled, extracted according to specifications and implemented as shown in Fig. 1.

In the model development, TYPE 109-TMY is used for the climate of Taxila (33.7463° N, 72.8397° E) incorporating TMY2 file which is generated from Meteonorm tool. Solar thermal system is used as heat source to regenerate desiccant wheel and generating vapors of

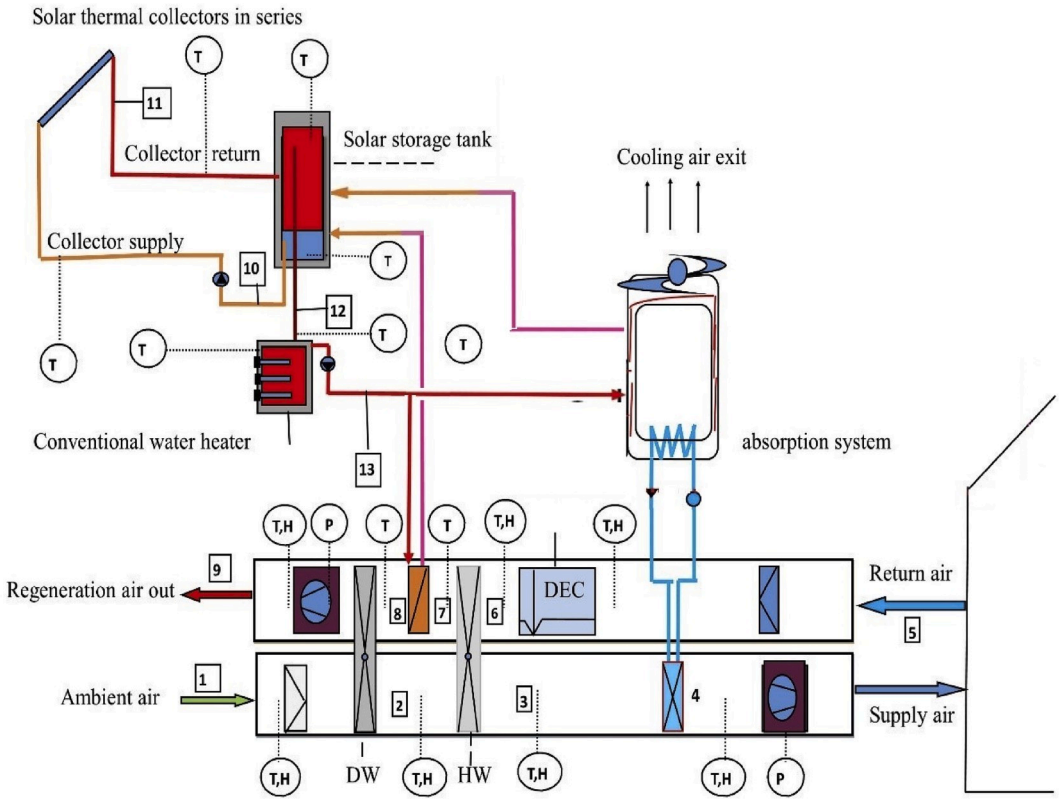


**Fig. 1.** Schematic diagram of IADS.

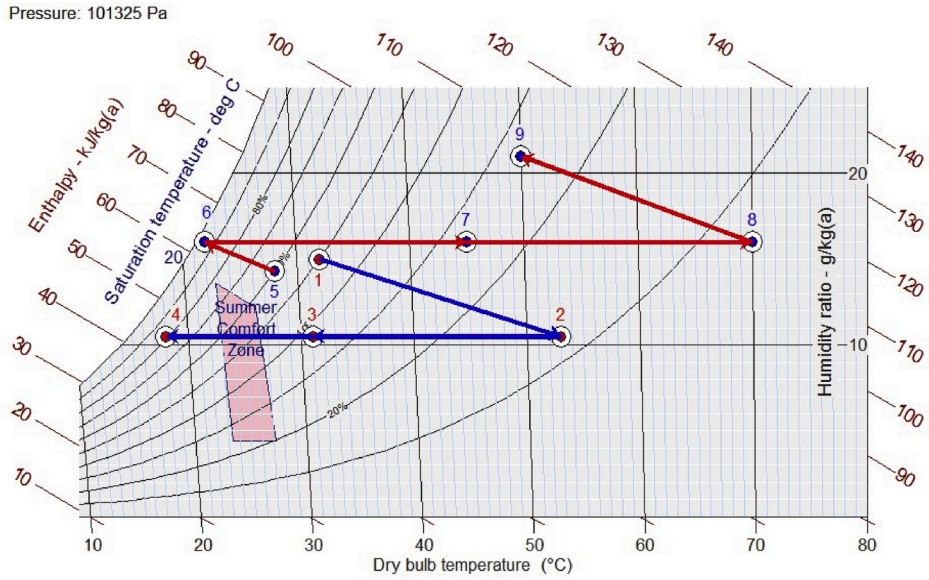


**Fig. 2.** Psychometric representation of the system processes.

refrigerant in absorption system. Conditioned air is supplied to the building under consideration where both type of loads sensible (peak sensible load of 10.94 kW) and latent load (peak latent load of 4.44 kW) are applied. The IADS model developed in TRNSYS is shown in Fig. 3. Afterwards, other components are connected accordingly, and design variables of each component are set accordingly as mentioned in Table 1.

For model-based simulation technique the most important step is to set an appropriate controlling strategy for different components like pumps, boiler and other time base controlled components. In the current work, solar thermal source water flow pump is controlled by using GT (greater than) function through an equation i.e. GT($T_{c,o}$,$T_{c,i}$); when collector outlet temperature is greater than collector inlet temperature then controlling signal will be 1 otherwise it will be 0. Whereas, the flow pump that delivers hot water to absorption chiller is controlled by a time-based controlled function type 14 h and controlling signal will be 1 daily from 0900 to 1600 h i.e. simulation time for a day. Boiler operation is controlled by using a thermostat that ensure when boiler inlet temperature is less than 108 °C then controlling signal will be 1 otherwise it will be 0.

### 3.1. Desiccant wheel model

In the proposed IADS, the desiccant wheel is key component that has been modeled (TYPE 683) through equations developed by Howe and Jurinak based on isopotential lines (F1 and F2) for silica gel [38].

$$F1 = \frac{-2865}{T^{1.490}} + 4.344\omega^{0.8624} \tag{1}$$

$$F2 = \frac{T^{1.490}}{6360} - 1.127\omega^{0.07969} \tag{2}$$

Furthermore, Banks modified F1 and F2 for non-idealities in the system by two factors called $\varepsilon_{F1}$ and $\varepsilon_{F2}$ and given as:

$$\varepsilon_{F1} = \frac{F1_D - F1_P}{F1_R - F1_P} \tag{3}$$

$$\varepsilon_{F2} = \frac{F2_D - F2_P}{F2_R - F2_P} \tag{4}$$

Where D represents the actual outlet state.

### 3.2. Absorption chiller

To model the chilled water system, hot water fired single effect absorption chiller component (TYPE 680) from TRNSYS library was used. The amount of energy removed from chilled water in order to bring the water up to required set point temperature is given as:

$$\dot{Q}_{removed} = \dot{m}_{chw}\, Cp_{chw}\left(T_{chw,i} - T_{chw,\,sp}\right) \tag{5}$$

The energy balance is given as:

$$\dot{Q}_{cw} = \dot{Q}_{chw} + \dot{Q}_{hw} + \dot{Q}_{aux} \tag{6}$$

The COP of the device is calculated as:

$$\mathrm{COP} = \frac{\dot{Q}_{chw}}{\dot{Q}_{hw} + \dot{Q}_{aux}} \tag{7}$$

### 3.3. Solar thermal collector

TRNSYS TYPE 1b is used to model the operation of a flat plate solar thermal collector. To model this type the results provided by the user from standard test of a quadratic curve that is efficiency vs ratio of the difference between fluid temperature and ambient temperature to the incident radiation ($\frac{\Delta T}{G}$).

The following efficiency equation simulates the working of the solar collector [39].

$$\eta = a_0 - a_1\left(\frac{\Delta T}{G}\right) - a_2\frac{(\Delta T)^2}{G} \tag{8}$$

Three parameters $a_0$, $a_1$ and $a_2$ are selected according to ASHRAE standards rated by SRCC [40].

Typical values of these parameters are shown in Table 2.

### 3.4. Building model

The considered load of 15.38 kW represents a typical office building. The building model (Type 690) used in the current study is that in which the user imposes a load and estimated thermal capacitance of the building that includes building materials capacitance, conditioned air and furnishing are determined. The Building model then gives the resultant humidity ratio and temperature of the conditioned space and

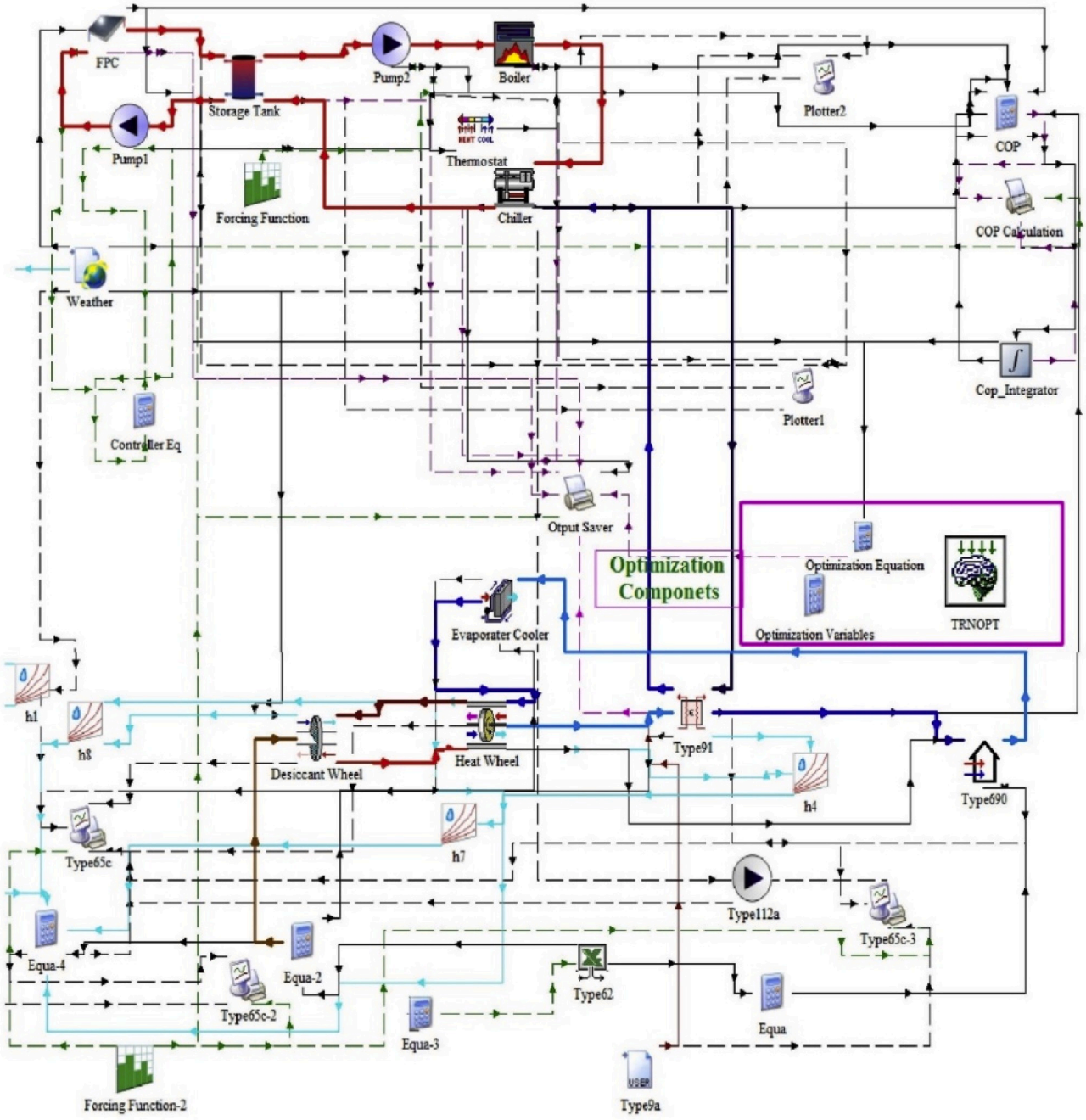


**Fig. 3.** TRNSYS Model coupled with GenOpt for Simulation and Optimization of IADS.

**Table 1**
The System design Specifications.

| Parameter | Value |
|---|---|
| System's Capacity (kW) | 5.5 |
| Dehumidifier Effectiveness F1 | 0.08 |
| Dehumidifier Effectiveness F2 | 0.95 |
| *Air volume flow rate (CFM)* | 450 |
| Peak Sensible Load (kW) | 10.94 |
| Peak Latent Load (kW) | 4.44 |
| Area of flat plate collector ($m^2$) | 20 |
| Storage Tank Volume ($m^3$) | 10 |

**Table 2**
Efficiency parameters for flat plate solar collector.

| $a_o$ | $a_1$ kJ $hr^{-1}$ $m^{-2}K^{-1}$ | $a_2$ kJ$hr^{-1}$ $m^{-2}K^{-2}$ | *Tested Flow rate* kg $hr^{-1}$ $m^{-2}$ | Incidence Angle Modifier *(IAM)* |
|---|---|---|---|---|
| 0.80 | 13 | 0.05 | 40 | 1–0.2(1/cosθ - 1) |

the back calculation based on differential equations.

## 4. Optimization of the integrated system

In the current study, optimization is performed at two levels, first using Hooke-Jeeves algorithm to optimize system $COP_{th}$ and secondly optimizing solar fraction using TRNOPT. Hooke-Jeeves algorithm is

used because this algorithm only optimizes continuous variables and intelligently select iteration to approach optimized objective function. First level optimizes the standalone absorption chiller based on well-defined constraints i.e. generator temperature must remain ≥108 °C. $COP_{th}$ of absorption system and solar fraction are two objective functions for optimization of first level. Whereas, second level optimizes IADS based on two additional constraints: (1) zone temperature must remain ≤27 °C; (2) regeneration temperature must be ≤ 70 °C. Overall $COP_{th}$ of IADS and solar fraction are the objective functions for optimization of second level. A comprehensive flow chart of optimization for both levels is shown in Fig. 4. Constraints in the model are handled using penalty function technique. Whenever constraint doesn't meet the set criteria for any iteration, then a penalty is added to the objective function and GenOpt discarded that value from optimum value of the objective function. When it is required to maximize a function then just a negative sign with the function works as to maximize the function in GenOpt. Optimization variables with range are listed in Table 3.

For level 1:
Min(f) = – (COP of the system).
Min(f) = – (Solar Fraction).
Constraint Handled: $T_g \geq 108$ °C
For Level 2:
Min(f) = – (COP of the system).
Min(f) = – (Solar Fraction).
Constraint Handled: $T_z \leq 27$ °C & $T_{reg} \leq 70$ °C
Parameters for Hooke-Jeev's algorithm for optimization are [41]:

1. Initial Mesh Size Exponent = 0

**Table 3**
Optimization variables range.

| Variable | Range | Step Value |
|---|---|---|
| $A_c$ ($m^2$) | 2–18 | 1 |
| $\dot{m}_{pump1}$ (kg/h) | 100–2000 | 100 |
| $\dot{m}_{pump2}$ (kg/h) | 100–3000 | 100 |
| $V_t$ ($m^3$) | 1–10 | 0.5 |
| $T_{cw,i}$ (°C) | 25–35 | 1 |
| $T_{ch,sp}$ (°C) | 5–10 | 0.5 |
| $\omega_{sp}$ (g/kg) | 5–12 | 0.5 |
| $\dot{m}_{cw}$ (kg/h) | 100–3000 | 100 |
| $\dot{m}_{chw}$ (kg/h) | 100–2000 | 100 |

2. Mesh Size Divider = 2
3. Maximum Number of Step Reduction = 4
4. Mesh Size Exponent Increment = 1

## 5. Validation of the simulation model of the integrated system

The simulation model of IADS is validated with a simulation study in which desiccant system was integrated with a vapor compression system [11]. Moreover another simulation study in which desiccant system integrated with M-cycle using indirect evaporative cooler [32] and experimental study of desiccant system integrated with M-cycle with indirect evaporative cooler [42] are also considered for comparison. Since the developed simulated model is based on standard validated components from the TRNSYS library, the mathematical models are well calibrated and the components thereby adopted are utilized in their

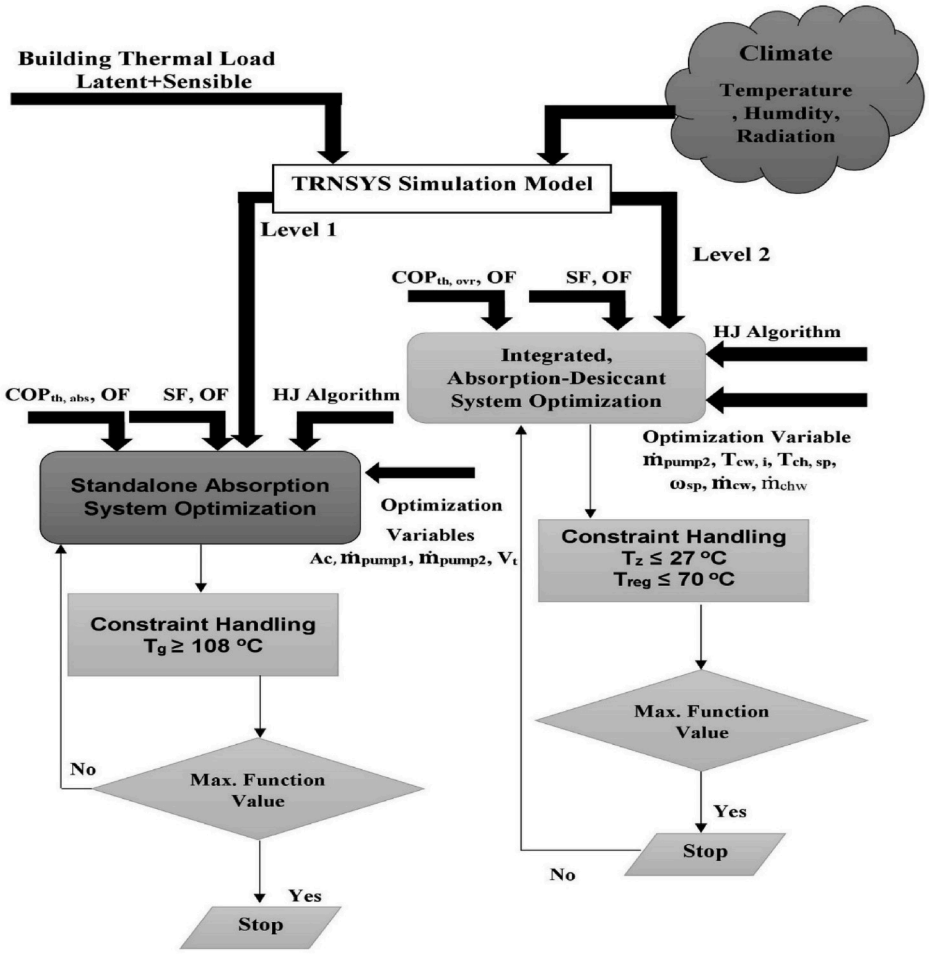


**Fig. 4.** Flow chart of Optimization.

ranges specified. The integrated model is also simulated at the test conditions of some of the previously published experimental data sets in order to ensure that the simulations results are reliable and the composition, methodology as well as scheme produces validated results. In this regard, the effect of ambient air humidity ratio and ambient temperature on supply air temperature for current and published studies is shown in Fig. 5. It can be observed that variation of supply air temperature at same inlet conditions for current study and a published study [11] is within an average of 5% deviation which is well within acceptable range. With the increase in the ambient temperature, the variations of supply temperatures at different ambient humidity ratios show slight increase in supply temperature. It is pertinent to mention that the experimental data of [11] used mechanical absorption system. Still both hybrid systems show significantly neat comparison in terms of achieving desired supply conditions with same ambient conditions. This indicates that the components, methodology and the simulation strategy achieved desired output.

However, there is a notable difference in supply air temperature while comparing the simulated results and the data produced in two published studies of [32,42]. The variations are notable since the previously published studies used desiccant system which is integrated with M-cycle using multi-stage indirect evaporative cooler which results in significantly higher supply air temperature compared to other hybrid systems. It can be concluded that proposed IADS in the current study is capable of providing much low supply temperature to ensure required thermal comfort.

## 6. Performance evaluation parameters

Performance evaluation of IADS is determined by different parameters including system thermal and electric COP, solar fraction, solar gain, auxiliary gain, auxiliary energy utilization, sensible energy, latent energy, and sensible heat factor [21,27].

The heat gain form solar energy is determined by:

$$Q_{sol} = \dot{m}_{1,w,c}.C_{p,w}.(T_{co} - T_{ci}) \tag{9}$$

The heat gain from auxiliary source is determined as:

$$Q_{aux} = \dot{m}_{2,w}.C_{p,w}.(T_{bo} - T_{bi}) \tag{10}$$

The total heat energy is formulated as;

$$Q_{tot,i} = Q_{sol} + Q_{aux} \tag{11}$$

The solar fraction is calculated as:

$$SF = \frac{Q_{sol}}{(Q_{sol} + Q_{aux})} \tag{12}$$

The auxiliary energy utilized is formulated as:

$$E_{aux} = \frac{Q_{aux}}{(Q_{sol} + Q_{aux})} \tag{13}$$

The sensible heat capacity, latent heat capacity and sensible heat factor (SHF) of IADS are calculated as:

$$Q_{sen} = C_{p,a}.\dot{m}_a.(T_{s,a,i} - T_{s,a,o}) \tag{14}$$

$$Q_{lat} = H.\dot{m}_a.(\omega_{p,a,i} - \omega_{p,a,o}) \tag{15}$$

$$SHF = \frac{Q_{sen}}{Q_{lat} + Q_{sen}} \tag{16}$$

The thermal coefficient of performance ($COP_{th}$) of systems is calculated as:

$$COP_{d,th} = \frac{\dot{m}(h_{amb} - h_{ec,out})}{Q_{reg,in}} \tag{17}$$

$$COP_{ovr,th} = \frac{\dot{m}(h_{amb} - h_{hx,out})}{Q_{reg,in}} \tag{18}$$

The electric coefficient of performance (COP) of systems is calculated as:

$$COP_{d,elc} = \frac{\dot{m}(h_{amb} - h_{ec,out})}{E_{elc,DAC}} \tag{19}$$

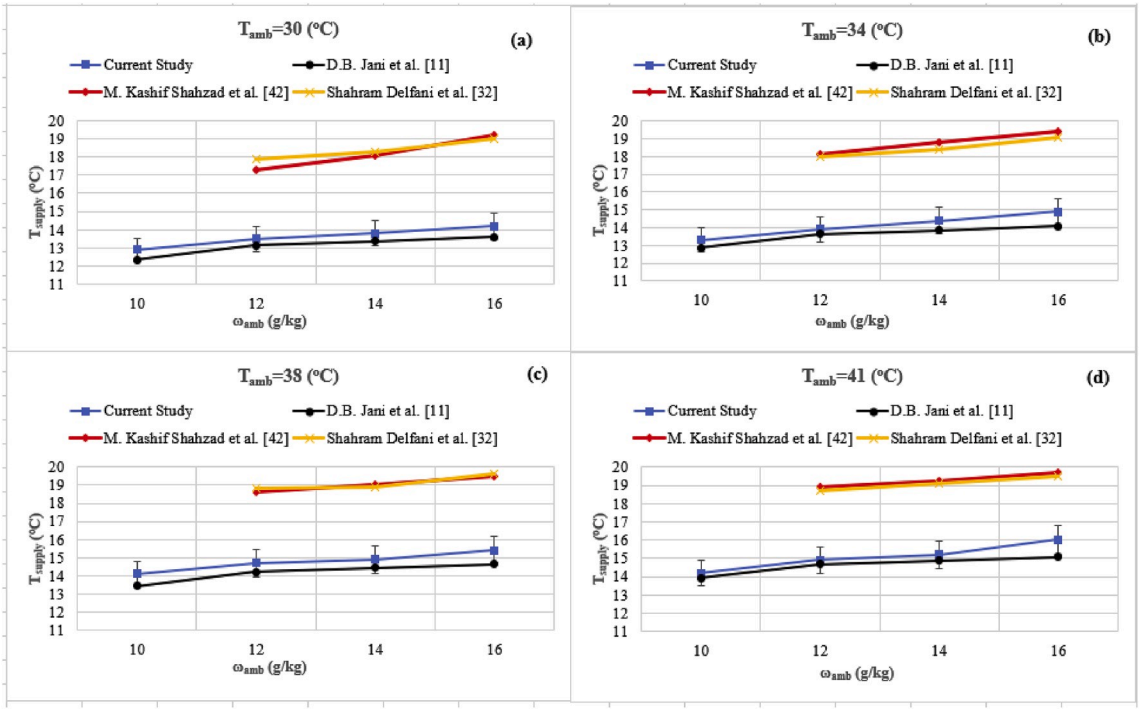


**Fig. 5.** Model validation (a) $T_{amb}$ = 30 °C, (b) $T_{amb}$ = 34 °C, $T_{amb}$ = 38 °C and $T_{amb}$ = 41 °C.

$$COP_{ovr,elc} = \frac{\dot{m}(h_{amb} - h_{hx,out})}{E_{elc,IADS}} \quad (20)$$

## 7. Results and discussion

Results of local climate variation (including variation of temperature, solar radiation and building load), performance analysis of solar thermal, standalone absorption, desiccant and IADS, two level optimization and finally effect of separate load management are presented in this section.

### 7.1. Climate variation

In the current study, a subtropical climate i.e. Taxila 33.7463° N, 72.8397° E is considered for the analysis of both standalone and integrated systems. The average global radiation and diffused radiation for summer season for the selected climate is about 609.77 W/m$^2$ and 273.20 W/m$^2$, respectively. Hourly variation is shown in Fig. 6 and variation in ambient temperature is shown in Fig. 7.

The building thermal load is applied through an hourly based load profile in terms of sensible load and latent loads for cooling season as shown in Fig. 8. Sensible to latent load ratio is also presented along with load profile. It can be observed that the ratio varies from 0 to 10 from April to August. Peak sensible load is 10.94 kW and peak latent load is 4.44 kW.

### 7.2. Performance analysis of solar thermal system

The solar thermal system is key sub-system as it provides the required driving force to operate the system thermally. Fig. 9 indicates the profile of monthly average solar fraction for the whole cooling season. It can be observed that the solar fraction in July is maximum as the solar gain in this month is maximum and auxiliary energy required at that time is minimum. The average value of solar fraction varies from 53% to 59% for the season.

### 7.3. Performance analysis of standalone and integrated systems

In the current work, initially, the performances of standalone absorption chiller, standalone desiccant system and IADS are investigated for the whole cooling season starting from April to August. The transient simulations results in terms of useful solar energy gain of 60928 kWh$_{th}$, energy consumption of auxiliary source of 15747 kWh$_{th}$ with solar fraction of 56.20%, and COP$_{th}$ of 1.49 for the specified cooling season are given in Table 4. In addition, it was determined that auxiliary energy

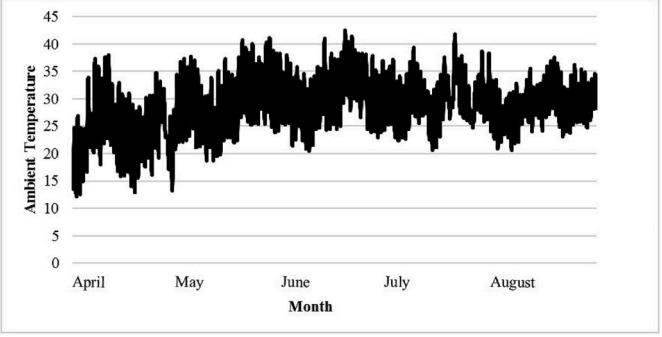


**Fig. 7.** Variation in ambient temperature.

consumption is around 25% of useful solar gain to achieve the required T$_{reg}$ of 70 °C.

Variation in different air temperatures and solar radiations for a typical summer day is shown in Fig. 10. The term typical day/design-day is used frequently in the HVAC industry. Design-day is typically used to describe a period with extreme outdoor conditions usually correspond to the maximum solar conditions that a HVAC system is designed to cater and subsequently maintain the desired indoor temperature and humidity to ensure thermal comfort. Therefore, in the current work, 25$^{th}$ of June 2019 is considered as a typical summer day for the selected climate. Ambient temperature (T$_{amb}$) varies from 31.9 °C to 36 °C and collector outlet temperature varies from 83 to 97 °C from 0900 to 1600 h. At around 1300 h the collector outlet temperature is maximum as at that time solar gain is maximum with auxiliary energy requirement at that time is minimum; when air regeneration temperature (T$_{reg}$) is almost maintained around 70 °C. Moreover, it can be observed that the resulted supply air temperature (T$_{sa}$) remains almost constant between 13 to 14 °C and building indoor zone temperature (T$_z$) also remains around 23–24 °C from 0900 to 1600 h which ensures thermal comfort to meet the given building load. Solar radiation varies from 0900 to 1600 h and maximum solar radiation is 965 W/m$^2$ at 1200 h.

Moreover, COP$_{elc}$ is also determined to further compare the both systems as shown in Fig. 11. It can be observed that COP$_{th}$ of IADS is 88.24% higher than the COP$_{th}$ of DAC. The COP$_{elc}$ of IADS is 151.27% higher than the COP$_{elc}$ of DAC. In the month of June both parameters are at their peak values due to maximum solar energy gain. Additionally, another reason is that the cooling effect produced by IADS and DAC is maximum at that time. However, cooling effect for IADS is greater than that DAC throughout the cooling season. Thus, both COP$_{elc}$ and COP$_{th}$ of IADS are greater than that of DAC. Therefore, it can be concluded that

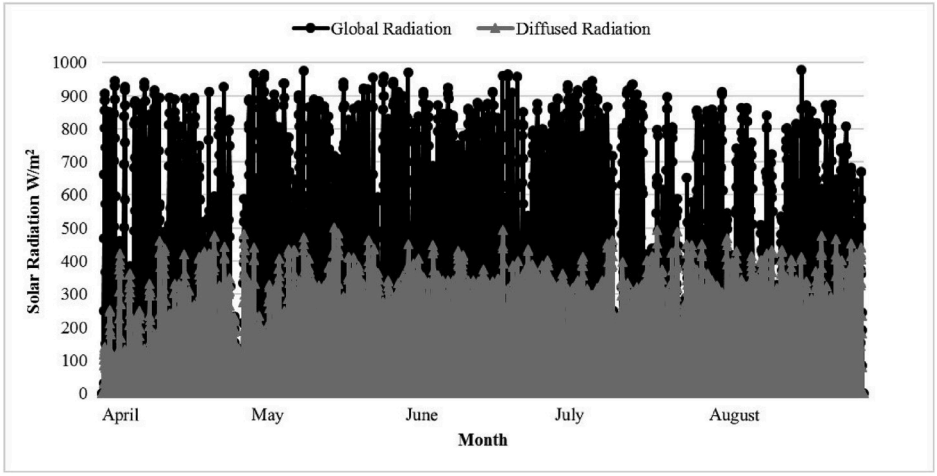


**Fig. 6.** Hourly variation of global and diffused radiation of Taxila.

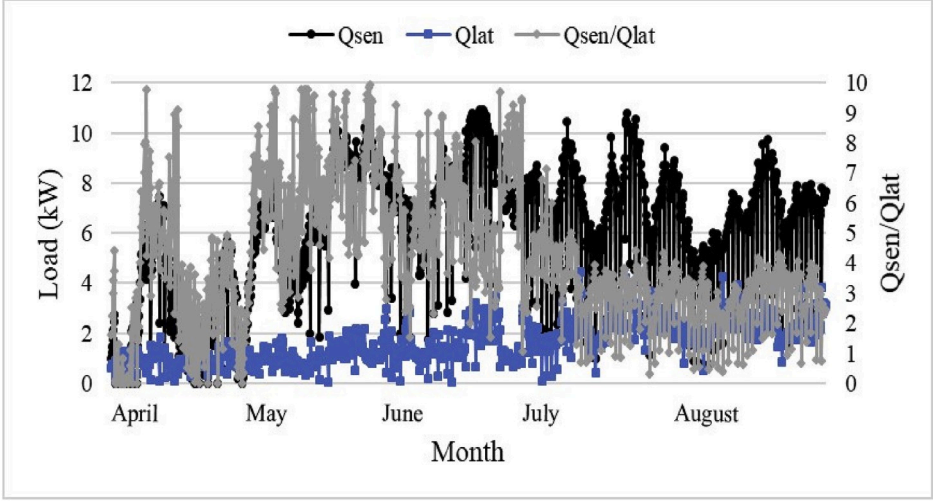


**Fig. 8.** Load profile for cooling season.

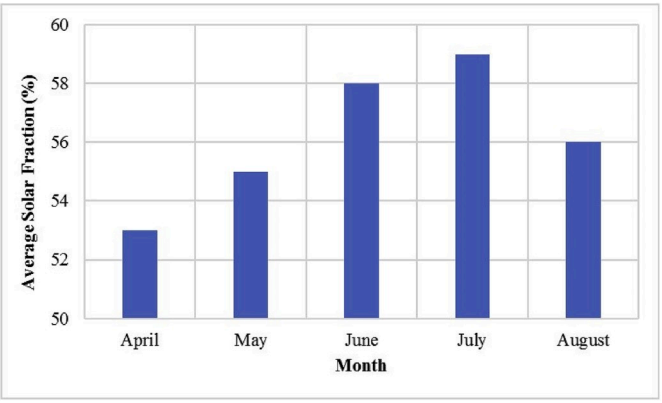


**Fig. 9.** Profile of monthly average solar fraction for whole season.

**Table 4**
Simulation results for whole cooling season.

| Parameter | Value |
|---|---|
| Useful Solar Energy gain for whole season ($kWh_{th}$) | 60928.00 |
| Auxiliary Energy Consumption for whole season ($kWh_{th}$) | 15747.04 |
| Seasonal average value of Solar Fraction (%) | 56.20 |
| Seasonal average value of $COP_{th}$ | 1.49 |

IADS performs much better which results in significant energy savings.

### 7.4. Optimization of the integrated system

Optimization is performed at 02 levels: (1) optimization of standalone system (level 01), (2) and optimization of the integrated (level 02) system. The optimization outcomes of both levels are summarized in Table 5. It can be seen that optimal value of objective function SF is 57.50% of solar thermal system. Afterwards, the optimized solar thermal system with optimal values of Ac, $\dot{m}_{pump1}$, $\dot{m}_{pump2}$ and $V_t$ is then coupled with absorption system which resulted in the optimal $COP_{th}$ of 0.56. Whereas, the level 02 optimization resulted SF of 56.25% which is slightly less than standalone system because both absorption and desiccant systems are being driven by the solar thermal system. However, optimal $COP_{th}$ of IADS is 1.52 which is significantly higher than the standalone system due to high system cooling capacity.

### 7.5. Effect of separate load management

It is analyzed during the study that the performance of IADS also depends upon the building sensible and latent loads ratio. The effect of variation of sensible and latent load on $COP_{th}$ of standalone desiccant system and IADS is indicated in Fig. 12. Sensible load is kept constant at 5 kW and latent load is varied from 1 kW to 10 kW to assess the effect of latent load variation on COP of the system. As the load ratio varies from 5 to 0.5, $COP_{th}$ of conventional desiccant air-conditioning system remains almost constant at 0.75 and $COP_{th}$ of IADS decreases slightly from 1.55 to 1.27 but still higher than the standalone system.

Therefore, in the current study, the suitability of both systems is further analyzed in term of effect of load variation on required regeneration heat as depicted in Fig. 13. It can be observed that regeneration heat remains almost same as far as load varies from 5 to 0.5 for conventional desiccant system. But in case of IADS, required regeneration heat increases with decrease in ratio of loads. When ratio of sensible load to latent load is greater than 0.75 i.e. 43% sensible load and 57% latent load, the required regeneration heat for IADS is less than DAC. Whereas, the required regeneration heat for conventional desiccant system is lower than the integrated system for ratio of loads less than 0.75. Thus, solar thermal source is needed to be carefully designed related to building load ratio to take the advantages of the integrated system.

The building variation is also commonly presented in terms of Sensible Heat Ratio. Therefore, effects of monthly average sensible heat factor for IADS for whole cooling season is analyzed as shown in Fig. 14. Sensible heat factor is varied from 0.4 to 0.9. In April the value of SHF is maximum and in August its value is minimum. The reason is that in April the system handled more sensible load as compared to latent load while in August system handles more latent load compared to sensible load.

Fig. 15 shows thermal energy flow of solar thermal source and auxiliary source of IADS and sensible heat factor for the typical summer day. It can be observed that 12 p.m.–2 p.m. the solar energy gain is much higher and subsequently the axillary energy requirement is very low at that time. The sensible heat factor varies from 0.4 to 0.51 from 9 a.m. to 4 p.m. for the specified day.

## 8. Conclusion

In the current work, thermal load management in terms of separate handling of sensible and latent loads through an integrated absorption and desiccant system is evaluated through a model-based simulation and optimization approach by coupling TRNSYS with GenOpt. It has been observed that the proposed integrated system is more efficient compared

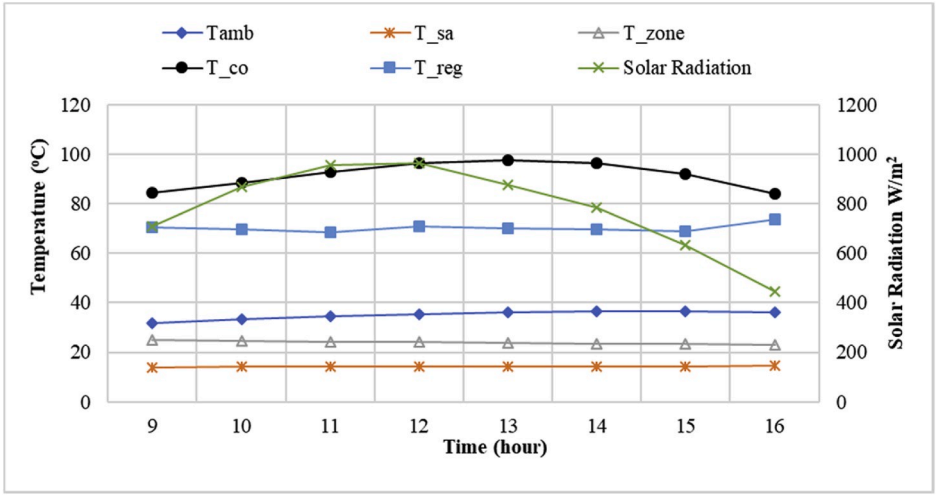


**Fig. 10.** Supply air temperature, zone temperature, ambient temperature, collector outlet temperature and regeneration temperature of a typical day of the summer.

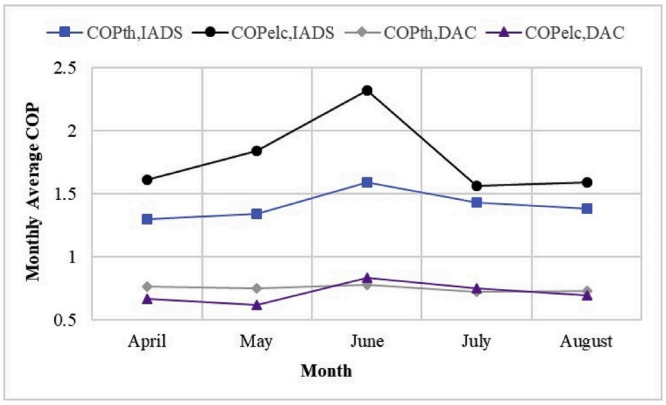


**Fig. 11.** Thermal and electric COP of standalone desiccant and IADS.

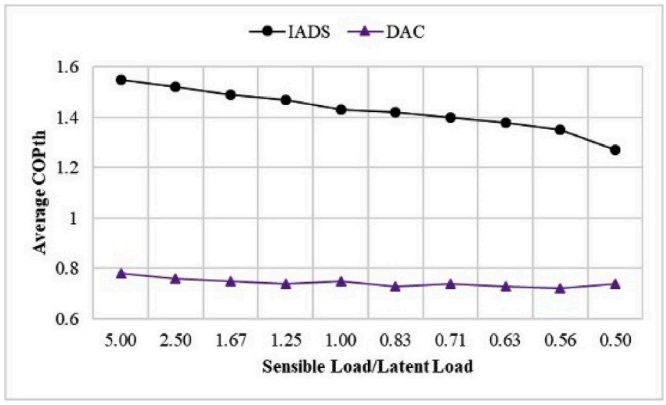


**Fig. 12.** Effect of load variation on COP of standalone desiccant system and IADS.

**Table 5**
Optimum values for both levels of optimization.

| Level:1 | | Level:2 | |
|---|---|---|---|
| **1.OF: SF** | | **1.OF: SF** | |
| SF (%) | 57.50 | SF (%) | 56.25 |
| $A_c$ ($m^2$) | 18 | $\dot{m}_{pump2}$ (kg/h) | 3000 |
| $\dot{m}_{pump1}$ (kg/h) | 800 | $T_{cw,i}$ (°C) | 30 |
| $\dot{m}_{pump2}$ (kg/h) | 2280 | $T_{ch,sp}$ (°C) | 7 |
| $V_t$ ($m^3$) | 1.5 | $\omega_{sp}$ (kg/kg) | 0.008 |
| **2.OF: $COP_{th,\ abs}$** | | $\dot{m}_{cw}$ (kg/h) | 2160 |
| $COP_{th,\ abs}$ | 0.55 | $\dot{m}_{chw}$ (kg/h) | 980 |
| Ac ($m^2$) | 20 | **2.OF: $COP_{th,\ ovr}$** | |
| $\dot{m}_{pump1}$ (kg/h) | 800 | $COP_{th,\ ovr}$ | 1.52 |
| $\dot{m}_{pump2}$ (kg/h) | 2850 | $\dot{m}_{pump2}$ (kg/h) | 2630 |
| $V_t$ ($m^3$) | 1.5 | $T_{cw,i}$ (°C) | 30 |
| | | $T_{ch,sp}$ (°C) | 7 |
| | | $\omega_{sp}$ (kg/kg) | 0.0085 |
| | | $\dot{m}_{cw}$ (kg/h) | 2220 |
| | | $\dot{m}_{chw}$ (kg/h) | 905 |

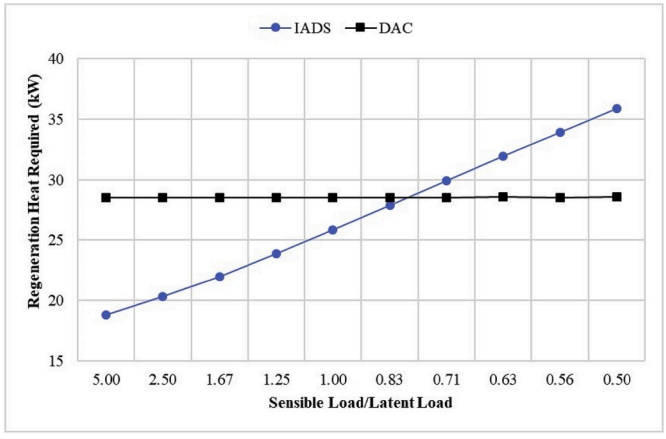


**Fig. 13.** Effect of load variation on Regeneration heat requirements of standalone desiccant system and IADS.

to standalone desiccant system for air-conditioning applications. Initially, the simulation model of IADS is validated with the similar hot and humid climate. Then, optimization of the integrated system was performed by considering appropriate system constraints to ensure that the required building load is achieved to attain the thermal comfort. The resulted optimized values of solar fraction are 56.25% and 57.50%; while, the optimized value of $COP_{th}$ are 1.52 and 0.55 for the integrated and standalone absorption system, respectively. The effect of load variation on required regeneration heat for both integrated and standalone systems is also analyzed and a critical load ratio of 0.75 is observed.

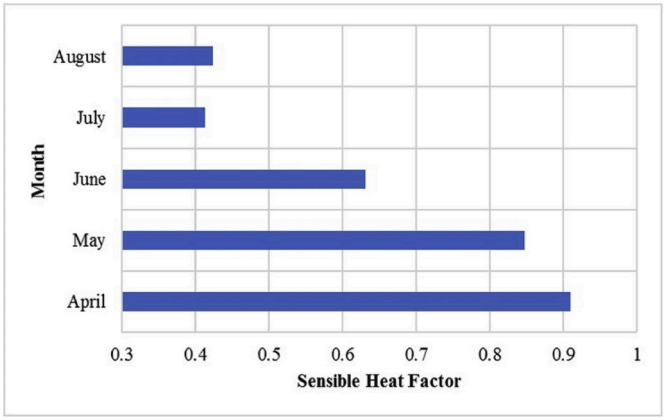


**Fig. 14.** Profile of monthly average sensible heat factor.

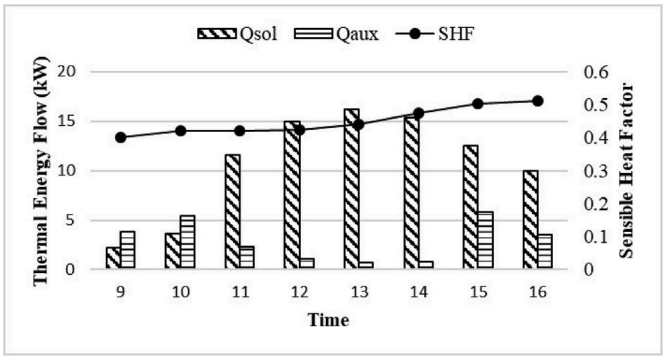


**Fig. 15.** Thermal Energy flow of IADS for a typical summer day.

## Declaration of competing interest

The authors declare that they have no known competing financial interests or personal relationships that could have appeared to influence the work reported in this paper.

## CRediT authorship contribution statement

**Muhammad Farhan Habib:** Conceptualization, Methodology, Software. **Muzaffar Ali:** Methodology, Software, Investigation. **Nadeem Ahmed Sheikh:** Writing - original draft, Formal analysis, Writing - review & editing. **Abdul Waheed Badar:** Visualization. **Sajid Mehmood:** Software, Validation, Writing - review & editing.

## Acknowledgements

The authors are thankful to Higher Education Commission of Pakistan for providing funding under Technology Development Fund.

## Appendix A. Supplementary data

Supplementary data to this article can be found online at https://doi.org/10.1016/j.jobe.2020.101279.

## References

[1] X. Tang, Depletion of fossil fuels and anthropogenic climate change — a review 52 (2013) 797–809.
[2] M.Z. Jacobson, Review of Solutions to Global Warming , Air Pollution , and Energy Security †, 2009, pp. 148–173.
[3] IEA, "International Energy Agency.".
[4] L. Pe, A review on buildings energy consumption information ', Energy Build. 40 (2008) 394–398.
[5] D.B. Jani, M. Mishra, P.K. Sahoo, A critical review on application of solar energy as renewable regeneration heat source in solid desiccant – vapor compression hybrid cooling system, J. Build. Eng. 18 (2018) 107–124, no. March.
[6] P. Mazzei, F. Minichiello, D. Palma, HVAC dehumidification systems for thermal comfort: a critical review, Appl. Therm. Eng. 25 (5–6) (2005) 677–707.
[7] K.F. Fong, T.T. Chow, C.K. Lee, Z. Lin, L.S. Chan, Solar hybrid cooling system for high-tech offices in subtropical climate – radiant cooling by absorption refrigeration and desiccant dehumidification, Energy Convers. Manag. 52 (8–9) (2011) 2883–2894.
[8] D.B. Jani, M. Mishra, P.K. Sahoo, Performance analysis of a solid desiccant assisted hybrid space cooling system using TRNSYS, J. Build. Eng. 19 (2018) 26–35, no. April.
[9] A. Aliane, S. Abboudi, C. Seladji, B. Guendouz, An illustrated review on solar absorption cooling experimental studies, Renew. Sustain. Energy Rev. 65 (2016) 443–458.
[10] W.B. Hwang, S. Choi, D.Y. Lee, In-depth analysis of the performance of hybrid desiccant cooling system incorporated with an electric heat pump, Energy 118 (2017) 324–332.
[11] D.B. Jani, M. Mishra, P.K. Sahoo, Performance studies of hybrid solid desiccant – vapor compression air-conditioning system for hot and humid climates, Energy Build. 102 (2015) 284–292.
[12] K.F. Fong, C.K. Lee, T.T. Chow, Z. Lin, L.S. Chan, Solar hybrid air-conditioning system for high temperature cooling in subtropical city, Renew. Energy 35 (11) (2010) 2439–2451.
[13] A. Al-Alili, Y. Hwang, R. Radermacher, I. Kubo, A high efficiency solar air conditioner using concentrating photovoltaic/thermal collectors, Appl. Energy 93 (2012) 138–147.
[14] A.E. Kabeel, M. Abdelgaied, R. Sathyamurthy, T. Arunkumar, Performance improvement of a hybrid air conditioning system using the indirect evaporative cooler with internal baffles as a pre-cooling unit, Alexandria Eng. J. 56 (4) (2017) 395–403.
[15] G. Angrisani, C. Roselli, M. Sasso, Experimental assessment of the energy performance of a hybrid desiccant cooling system and comparison with other air-conditioning technologies, Appl. Energy 138 (2015) 533–545.
[16] J. Guo, et al., Ground Coupled Photovoltaic Thermal (PV/T) Driven Desiccant Air Cooling, 2014 no. December.
[17] W. Su, X. Zhang, Thermodynamic analysis of a compression-absorption refrigeration air-conditioning system coupled with liquid desiccant dehumidification, Appl. Therm. Eng. 115 (2017) 575–585.
[18] L. Chen, Z. Yu, Research of a rotary desiccant wheel based hybrid air conditioning system with natural cold source, Procedia Eng. 205 (2017) 492–496.
[19] K.F. Fong, C.K. Lee, Investigation on hybrid system design of renewable cooling for office building in hot and humid climate, Energy Build. 75 (2014) 1–9.
[20] K.F. Fong, C.K. Lee, Investigation of separate or integrated provision of solar cooling and heating for use in typical low-rise residential building in subtropical Hong Kong, Renew. Energy 75 (2015) 847–855.
[21] K.F. Fong, T.T. Chow, Z. Lin, L.S. Chan, Simulation-optimization of solar-assisted desiccant cooling system for subtropical Hong Kong, Appl. Therm. Eng. 30 (2–3) (2010) 220–228.
[22] F. Calise, M.D. D'Accadia, L. Vanoli, Thermoeconomic optimization of solar heating and cooling systems, Energy Convers. Manag. 52 (2) (2011) 1562–1573.
[23] C.X. Jia, Y.J. Dai, J.Y. Wu, R.Z. Wang, Analysis on a hybrid desiccant air-conditioning system, Appl. Therm. Eng. 26 (2006) 2393–2400.
[24] H. Henning, T. Erpenbeck, C. Hindenburg, I.S. Santamaria, "The potential of solar energy use in desiccant cooling cycles Â nergie solaire dans les cycles de Utilisation potentielle de l ' e Á de À shydratant refroidissement a, Int. J. Refrig. 24 (2001) 220–229.
[25] M. Saghafifar, M. Gadalla, ScienceDirect Performance assessment of integrated PV/T and solid desiccant air-conditioning systems for cooling buildings using Maisotsenko cooling cycle, Sol. Energy 127 (2016) 79–95.
[26] K.F. Fong, T.T. Chow, C.K. Lee, Z. Lin, L.S. Chan, Advancement of solar desiccant cooling system for building use in subtropical Hong Kong, Energy Build. 42 (12) (2010) 2386–2399.
[27] G. Qadar, N. Ahmed, S. Ihtsham, S. Khushnood, Integration of solar assisted solid desiccant cooling system with e ffi cient evaporative cooling technique for separate load handling, Appl. Therm. Eng. 140 (2018) 696–706, no. May.
[28] F. Assilzadeh, S.A. Kalogirou, Y. Ali, K. Sopian, Simulation and optimization of a LiBr solar absorption cooling system with evacuated tube collectors, Renew. Energy 30 (8) (2005) 1143–1159.
[29] G. Fraisse, Y. Bai, N. Le Pierrès, T. Letz, Comparative study of various optimization criteria for SDHWS and a suggestion for a new global evaluation, Sol. Energy 83 (2) (2009) 232–245.
[30] A. Shirazi, R.A. Taylor, G.L. Morrison, S.D. White, A comprehensive, multi-objective optimization of solar-powered absorption chiller systems for air-conditioning applications, Energy Convers. Manag. 132 (2017) 281–306.
[31] R. Qi, L. Lu, Y. Huang, Parameter analysis and optimization of the energy and economic performance of solar-assisted liquid desiccant cooling system under different climate conditions, Energy Convers. Manag. 106 (2015) 1387–1395.
[32] S. Delfani, M. Karami, Transient simulation of solar desiccant/M-Cycle cooling systems in three different climatic conditions, J. Build. Eng. 29 (2020), 101152 no. December 2019.
[33] M.H. Mahmood, M. Sultan, T. Miyazaki, Experimental evaluation of desiccant dehumidification and air-conditioning system for energy-efficient storage of dried fruits, J. Build. Serv. Eng. Res. Technol. (2019), https://doi.org/10.1177/0143624419893660.

[34] T.M. Muhammad Hamid Mahmood, Muhammad Sultan, Significance of temperature and humidity control for agricultural products storage: overview of conventional and advanced options, Int. J. Food Eng. (2019) 1–21.
[35] M.H. Mahmood, M. Sultan, T. Miyazaki, "Solid desiccant dehumidification-based air-conditioning system for agricultural storage application : theory and experiments, J. Power Energy (2019) 1–14, vol. 0, no. 0.
[36] H. Niaz, M. Sultan, M.H. Mahmood, Z.M. Khan, Livestock application in Pakistan STUDY ON EVAPORATIVE COOLING ASSISTED DESICCANT AIR-CONDITIONING SYSTEM FOR LIVESTOCK APPLICATION IN Pakistan, Fresenius Environ. Bull. (2019), https://doi.org/10.5772/intechopen.88945 no. September.
[37] J.P.K.S.A. Klein, W.A. Beckman, J.W. Mitchell, J.A. Duffie, N.A. Duffie, T. L. Freeman, J.C. Mitchell, J.E. Braun, B.L. Evans, TRNSYS 16–A TRaNsient System Simulation Program, User Manual, Sol. Energy Lab. Madison Univ. Wisconsin-Madison, 2004.
[38] S.A. Klein, et al., TRNSYS 17 Volume 4 Mathematical Reference, 2012. *SEL (Solar Energy Lab. Univ. Wisconsin-Madison), TRANSSOLAR Energietechnik GmbH, CSTB (Centre Sci. Tech. Bâtiment), TESS* (Thermal Energy Syst. Spec.
[39] TRNSYS 17: A Transient System Simulation Program." Solar Energy Laboratory, University of Wisconsin, Madison, USA.
[40] ASHRAE, Solar Collectors and Photovoltaic in energyPRO, 2013, pp. 1–23, no. September.
[41] TESS Library, "Optimal Design with TRNSYS and GenOpt," (vol. TRNSYS Doc).
[42] M. Kashif Shahzad, M. Ali, N. Ahmed Sheikh, G. Qadar Chaudhary, M. Shahid Khalil, T.U. Rashid, Experimental evaluation of a solid desiccant system integrated with cross flow Maisotsenko cycle evaporative cooler, Appl. Therm. Eng. 128 (2018) 1476–1487.